New approach for severe marine weather study using satellite passive microwave sensing

Elizaveta V. Zabolotskikh,[1] Leonid M. Mitnik,[2] and Bertrand Chapron[3]

Received 30 April 2013; revised 6 June 2013; accepted 12 June 2013; published 9 July 2013.

[1] A methodology, based on model simulations and neural networks inversion, is proposed to jointly retrieve sea surface wind speed, sea surface temperature, atmospheric water vapor content, cloud liquid water content, and total atmospheric absorption at 10.65 GHz using Advanced Microwave Scanning Radiometer 2 measurements. In particular, estimation of the total atmospheric absorption at 10.65 GHz, which can be done with high accuracy due to the not so strong influence of liquid water and especially water vapor, helps to refine a new filter to considerably reduce masking ocean areas for severe weather systems, characterized by high wind speeds and moderate atmospheric absorption, appropriate for studying winter extratropical cyclone and polar low systems. A polar low case study has demonstrated significant improvement in the coverage of the ocean area available for geophysical retrievals: Only less than 1% of high wind speed pixels were masked comparatively to the 40–70% masking given by other methods. **Citation:** Zabolotskikh, E. V., L. M. Mitnik, and B. Chapron (2013), New approach for severe marine weather study using satellite passive microwave sensing, *Geophys. Res. Lett.*, *40*, 3347–3350, doi:10.1002/grl.50664.

1. Introduction

[2] One of the major applications of satellite passive microwave data is the study of marine severe weather systems [e.g., *Quilfen et al*., 2007]. Over the past decades, numerous algorithms have then been proposed to retrieve sea surface temperature (SST), sea surface wind speed (SWS), atmospheric total water vapor content (TWV), and cloud liquid water path (LWP), for the different available instruments.

[3] Under extreme conditions such as tropical cyclones, heavy precipitations, clouds, and high values of water vapor content can significantly mask the ocean contribution to brightness temperatures, TBs, mostly obtained at frequencies higher or equal to C band [e.g., *Reul et al*., 2012]. For winter extratropical cyclones at synoptic scale and mesoscale (polar lows), the atmospheric absorption is weaker and the ocean contribution to the TBs can be exploited and related to SWS variations. In this paper, we thus concentrate on the determination of a more accurate estimate of the atmospheric component of the TBs variations, which will allow retrieving SWS in much more cases than with conventional methods. Motivations are to refine both the weather filter mask and the retrieval of geophysical parameters.

[4] Some of the existing operational flags use predefined threshold values of retrieved cloud liquid water path LWP for nontransparent atmosphere masking. For example, Remote Sensing Systems, one of the major world data centers, processing satellite passive microwave measurement data and producing high-quality geophysical products [*Wentz and Meissner*, 2000], mask all the pixels with LWP exceeding 0.5 kg/m^2, considering these areas as too attenuated by the atmosphere. But without atmospheric water vapor content, LWP alone cannot be responsible for the atmospheric attenuation. Moreover, LWP is difficult to validate in the absence of in situ measurement data [*Alishouse et al*., 1990; *Jung et al*., 1998]. Other proposed atmospheric filters use either the threshold value of TB at 18.7 GHz, vertical polarization, or the predefined threshold on the polarization difference ΔT_B at 36–37 GHz (Japan Aerospace Exploration Agency science team used the threshold value of ΔT_B of 40 K to mask nontransparent atmosphere when producing Advanced Microwave Scanning Radiometer–EOS (AMSR-E) products) [*Japan Aerospace Exploration Agency*, 2005] to mask severe weather pixels. Both variables are certainly strongly dependent not only on the atmospheric properties but also on wind speeds, possibly leading to discard valuable observations.

[5] Hereafter, a novel absorption-based approach is considered and first applied to AMSR-2, the new Japanese radiometer on board GCOM-W1 satellite which substituted Aqua AMSR-E. As developed, this approach can also be used with other microwave radiometers in space. For AMSR-2 data, a threshold value on the retrieved total atmospheric absorption at 10.65 GHz is suggested to screen nontransparent atmospheres and to save masking large areas of high surface winds.

[6] The algorithm for the total atmospheric absorption at 10.65 GHz τ_{10} is jointly developed with SWS, TWV, and LWP retrieval algorithms. The approach is described in section 2 and applied to polar lows and extratropical cyclones in the North Atlantic, North Pacific, and Arctic regions. A case study is briefly considered in section 3 to demonstrate this new severe weather mask and SWS estimates and compared. Two other standard SWS products—one from the Japan Aerospace Exploration Agency (JAXA) GCOM-W1 Data Providing Service (AMSR-2) and the other from Remote Sensing Systems (http://www.ssmi.com/windsat/) (WindSat) are used for the comparison and demonstration of the advantages of the suggested approach.

Additional supporting information may be found in the online version of this article.

[1]Satellite Oceanography Laboratory, Russian State Hydrometeorological University, St. Petersburg, Russia.
[2]V. I. Il'ichev Pacific Oceanological Institute, Far-Eastern Branch of Russian Academy of Sciences, Vladivostok, Russia.
[3]Ifremer, Brest, France.

Corresponding author: E. V. Zabolotskikh, Satellite Oceanography Laboratory, Russian State Hydrometeorological University, Malookhtinsky Prospect 98, St. Petersburg 195196, Russia. (liza@rshu.ru)

0094-8276/13/10.1002/grl.50664

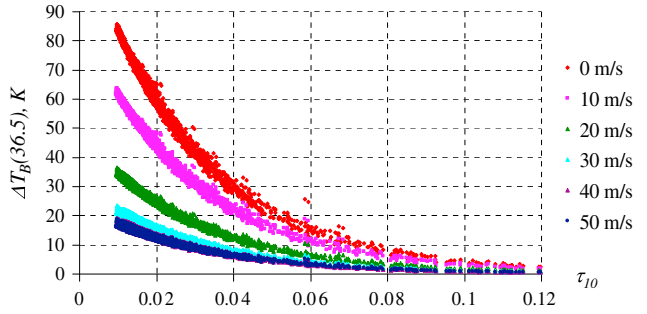

Figure 1. Simulated values of polarization difference ΔT_B at $\nu = 36.5$ GHz as a function of τ_{10} for different wind speeds from 0 to 50 m/s.

2. Approach

[7] Evaluation of the atmosphere-ocean system brightness temperatures $T_B^{V,H}$ and atmospheric absorption at 10.65 GHz τ_{10} has been previously described [*Mitnik and Mitnik*, 2003]. Restricted to nonprecipitating conditions, the model neglects the radiation scattering on large cloud particles and raindrops. Such an approximation is valid for microwave frequencies less than 37 GHz, for clear and cloudy atmosphere, and light rain up to ~2 mm/h [*Wentz and Spencer*, 1998]. Under such restrictions, the $T_B^{V,H}$ can be defined as

$$T_B{}^{V,H} = \chi^{V,H} \cdot Ts \cdot e^{-\tau \cdot \sec\theta} + T^{\uparrow}{}_B + T^{\downarrow}{}_B \cdot \left(1 - \chi^{V,H}\right) \cdot e^{-\tau \cdot \sec\theta} + T_{\cos}\left(1 - \chi^{V,H}\right) \cdot e^{-2\tau \cdot \sec\theta} \quad (1)$$

where $T_B^{V,H} = T_B^{V,H}(\nu,\theta)$ is the brightness temperature of the ocean-atmosphere system at frequency ν and incidence angle θ at vertical (V) and horizontal (H) polarization; $\chi^{V,H} = \chi^{V,H}(\nu,\theta,T_s,\mathrm{SWS},S)$ is the sea surface emissivity as a function of ν, θ, SST (T_s), SWS, and salinity S; $\tau(\nu)$ is the total atmospheric absorption at the frequency ν; $T^{\uparrow}{}_B(\nu,\theta)$ and $T^{\downarrow}{}_B(\nu,\theta)$ are the upwelling and downwelling brightness temperatures of the atmosphere, respectively; and $T_{\cos} = 2.73$ K is the brightness temperature of the cosmic background radiation.

[8] For the nonscattering approximation, both the atmospheric absorption and atmospheric constituents of the total microwave radiation are functions of vertical profiles of air pressure, temperature, humidity, and cloud liquid water content. These functions are evaluated using widely used and intensively validated models—[*Liebe and Layton*, 1987] for molecular oxygen and [*Turner et al.*, 2009] for water vapor absorption spectra. The ocean radiation $\chi^{V,H} \cdot Ts$ is governed by the ocean emissivity $\chi^{V,H}$ at horizontal and vertical polarizations, which for calm sea conditions is a function of frequency ν, incidence angle θ, sea surface temperature T_s, and salinity S [*Meissner and Wentz*, 2004]. Modeling of the wind influenced component of emissivity $\Delta\chi_W^{V,H}$ has undergone significant changes during the last several years [*Meissner and Wentz*, 2012]. The wind sensitivity, especially under gale wind conditions, greatly benefited from the data acquired by the Stepped Frequency Microwave Radiometer operating at $\nu = 5$–8 GHz [*Uhlhorn et al.*, 2007].

[9] Though the actual wind dependency of the ocean emissivity presents a sophisticated nonlinear function, a simple approximation can still be used to illustrate how strongly the polarization difference depends on the wind speed. Considering the two assumptions:

[10] 1. $\chi^{V,H}(\nu,\mathrm{SWS}) = \chi^{V,H}{}_0 + a^{V,H}(\nu) \cdot \mathrm{SWS}$. $a^H \gg a^V$ for AMSR-E and AMSR-2 ($\theta = 55°$) (valid up to about 15 m/s, then $a^{V,H}$ will be also the function of wind speed)

[11] 2. $T^{\uparrow}{}_B = T^{\downarrow}{}_B = T_{Batm}$, the polarization difference ΔT_B can be derived from (1). It consists of two parts: The first part corresponds to the calm sea surface (SWS = 0) and the second one depends on wind speed. Both parts decrease with the increase of total atmospheric absorption τ:

$$\begin{aligned}\Delta T_B = {} & \Delta T_B(\mathrm{SWS}) - \Delta T_B(\mathrm{SWS} = 0) \\ = {} & (T_s - T_{Batm})(\chi^V{}_0 - \chi^H{}_0)\, e^{-\tau\sec\theta} \\ & -(T_s - T_{Batm})(a^H - a^V)\mathrm{SWS}\tilde{n}e^{-\tau\sec\theta} \\ == {} & (T_s - T_{Batm}) \cdot e^{-t\sec}(\chi^V{}_0 - \chi^H{}_0 - (a^H - a^V)\mathrm{SWS})\end{aligned} \quad (2)$$

The component $T_{\cos}(\chi^V - \chi^H)\, e^{-2\tau\ \sec\theta}$ is less than 0.8 K and is neglected in (2).

[12] It is evident from (2) that the polarization difference decreases with the increase of wind speed for a given atmospheric absorption.

[13] To develop a new weather filter, computer simulations of the brightness temperatures were carried out for frequencies, polarization states, and angle of incidence of the AMSR-2 instrument for more than 2500 atmospheric and oceanic in situ data, using the radiative transfer model of the atmosphere-ocean system, described in details in *Bobylev et al.* [2010]. The only difference was incorporated concerning the wind-induced emissivity model taken from *Meissner and Wentz* [2012]. The data set was composed of radiosonde, meteorological, and hydrological (T_s and S) simultaneous measurements, taken by research vessels of the Far Eastern Research Hydrometeorological Institute (USSR/Russia), and modeled cloud liquid water profiles. Wind speed data are not correlated with the other geophysical parameters and were added randomly up to 60 m/s. The whole matched-up data set of geophysical parameters—TWV, LWP, total atmospheric absorption at 10.65 GHz τ_{10} (these parameters were calculated from the corresponding radiosonde reports), sea surface temperature Ts, SWS, and simulated values of T_B for AMSR-2 served as a database for model calculations and for the following algorithm development. To illustrate the dependency of the polarization difference ΔT_B on both SWS and τ_{10}, simulated ΔT_B(36.5 GHz) as a function of τ_{10} for different values of SWS is presented in Figure 1. High wind speeds lead to low values of ΔT_B even under clear atmosphere. So if masking is based on the usage of some threshold value on allowed ΔT_B, this can thus mask out valid pixels with extreme winds. For example, it can be seen from Figure 1 that according to model simulations, if SWS exceeds 20 m/s, ΔT_B is always less than 40 K (threshold, used previously by JAXA with AMSR-E), independently on the atmosphere properties. Usage of the threshold on total atmospheric absorption will allow masking only nontransparent atmospheres leaving unmasked the areas of high wind speeds, not accompanied by high values of atmospheric absorption.

[14] The whole database of geophysical parameters and corresponding simulated TBs was then divided between training and testing data sets. Standard neural networks (NNs) of multilayer perceptron type with feedforward backpropagation of errors and a single hidden layer of neurons were used to retrieve separately five parameters—TWV, LWP, SWS, SST, and τ_{10}. The detailed description

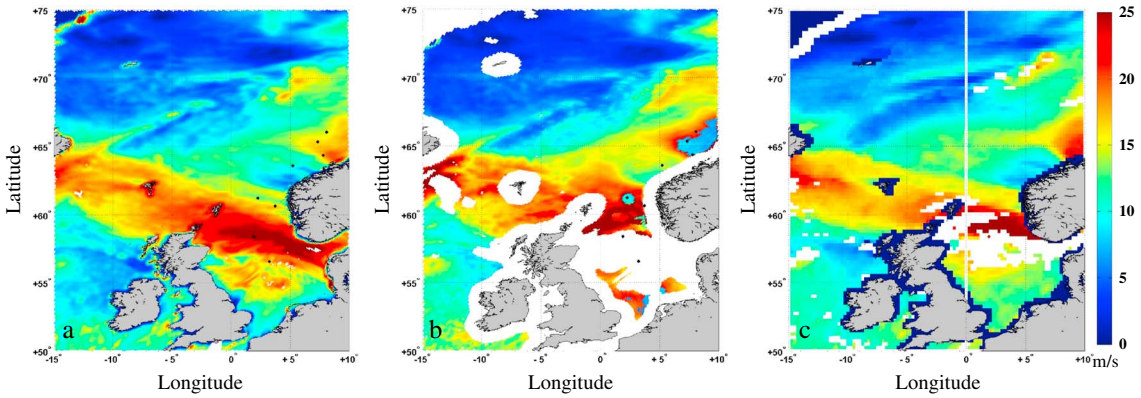

Figure 2. Wind speed fields in the polar low over the North Sea on 15 December 2012 retrieved from (a) AMSR-2 descending orbits (at 3:00 UTC and 1:25 UTC) using the NN algorithm; (b) GCOM-W1 JAXA SWS product (at 3:00 UTC and 1:25 UTC); and (c) WindSat SWS MF product (at 7:20 UTC). Black dots indicate platform positions.

of the algorithms and their validation is beyond the scope of this paper. The algorithms for TWV and LWP retrievals from SSM/I and AMSR-E and their careful validation are described in details in *Bobylev et al*. [2010]. The methodology for AMSR-E and AMSR-2 SWS and SST retrieval algorithm development is the same as described in the referenced paper, though the input TBs are different: SWS retrieval algorithm uses TBs at 18.7, 23.8, and 36.5 GHz; SST retrieval algorithm uses TBs at 6.9 and 10.65 GHz, both polarizations in each case. The validation of SWS and SST algorithms for AMSR-E data was done using JAXA database of more than 15,700 collocated AMSR-E and buoy measurements with the total retrieval error of about 1.2 m/s for SWS and 1 K for SST. For the recent AMSR-2 data, the algorithms still need to be validated using much more data than presented in the supporting information. The NN for the total atmospheric absorption τ_{10} consists of an input layer of brightness temperatures at 10.65, 18.7, and 23.8, both polarizations, single hidden layer of five neurons, and an output layer of a single output parameter τ_{10}. Numerical experiments were performed to select the optimal topology of NN. The absolute retrieval error is about 0.0013 (relative error is about 3%).

[15] The minimum value of $\tau_{10} \approx 0.01$ corresponds to total molecular oxygen absorption and cloudless atmosphere. Absorption by water vapor is small and the increase of τ_{10} is mainly due to water clouds. Cloud absorption τ_{cl} is proportional to LWP and depends on the effective cloud temperature t_{cl}. For example, $\tau_{cl}(10.65) = 0.0174$ at $t_{cl} = -10°C$, 0.0121 at $t_{cl} = 0°C$, and 0.0068 at $t_{cl} = +10°C$ for cloud with LWP = 0.5 kg/m^2. At LWP = 1.0 kg/m^2, the total cloud absorption will be two times higher. Large $\tau_{cl}(10.65)$ values are observed in heavy clouds. Usually, it is assumed that clouds with LWP $\geq$ 0.3–0.5 kg/m^2 are accompanied by precipitation.

[16] Further adjustments for calculated brightness temperature values, accounting for possible model inconsistencies and instrument calibration errors, are then derived by comparing measured and modeled T_Bs. Such comparisons were performed for the independent data set of cloudless radiosonde data, complemented with Metop-A advanced scatterometer (ASCAT)-derived wind data, collocated in time within 1 h and in space within 25 km with AMSR-2 measurement data. These additions are in agreement with those reported by various AMSR-2 research groups at the Joint PI Workshop of Global Environmental Observation Mission in the beginning of 2013.

3. Application to Marine Weather Systems With High Wind Speeds

[17] The proposed approach has been applied to study polar lows and extratropical cyclones over the North Atlantic and North Pacific Oceans and Arctic seas during 4 months —November 2012 to February 2013—using AMSR-2 measurements. All available complementary data including Metop-A ASCAT and Oceansat-2 Scatterometer (OSCAT) scatterometer wind fields, weather maps, buoy wind speed data, and radiosonde reports were then used to validate the geophysical parameters, obtained using the retrieved atmospheric absorption at 10.65 GHz τ_{10}.

[18] Geophysical parameter fields were compared with GCOM-W1 AMSR-2 standard products provided by Japan Aerospace Exploration Agency (JAXA) GCOM-W1 Data Providing Service (only SWS and SST are available for the moment—see https://gcom-w1.jaxa.jp) and with WindSat geophysical products, provided by Remote Sensing Systems (http://www.ssmi.com/windsat/). The area masked by existing weather filters (not taking into account the area close to land or ice or filtered by radio frequency interference filter) was calculated for these products and compared to estimates using the estimated τ_{10}. In general, a significant increase in the percentage of valid ocean pixels has been obtained. This is illustrated with AMSR-2 geophysical retrieved fields for a polar low over the North Sea on 15 December 2012 shown in Figure 2 for NN-retrieved SWS (a), GCOM-W1 JAXA standard SWS product (b), and RSS WindSat medium frequency (MF) SWS product (c). The percentage of the masked pixels for the selected area (latitudes 56°N–60°N, longitudes 0°E–4°E), associated with the polar low maximum development during 15 December at night, was equal to 45.6% for WindSat SWS MF product, 71.5% for GCOM-W1 JAXA SWS product, and only 0.3% for Neural Network SWS algorithm. Values for SWS, SST, LWP, and TWV can thus possibly be retrieved over the whole polar low area.

[19] More details can be found in the supporting information for the demonstration and applicability of the suggested approach. In particular, SWS algorithm performance over the

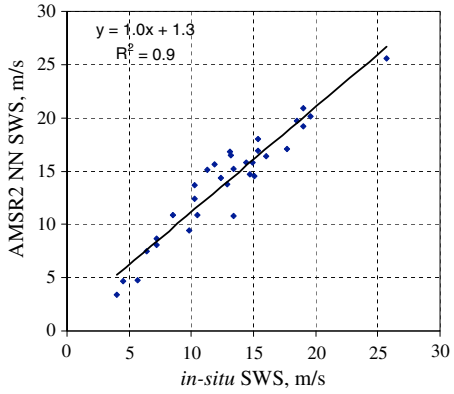

Figure 3. Scatterplot of AMSR-2 NN-retrieved versus in situ platform-measured SWS. Time difference between measurements is within half an hour.

area of the polar low development was done using eight platform weather station measurement data from the Norwegian Meteorological Institute (station positions are shown in Figure 3 as black dots). For the 14–15 December 2012 case, time differences between AMSR-2 and in situ measurements do not exceed 30 min to display an overall very good agreement (Figure 3).

4. Conclusion

[20] Efficient masking of the areas over the oceans, where geophysical parameter retrievals are objectively impossible due to nontransparent atmosphere, is still an important issue for satellite radiometer measurements. To go beyond present criteria, we suggest considering a more consistent approach based on the estimated value of the total atmospheric absorption. As demonstrated, this method can considerably increase unmasked ocean areas where the retrievals of sea surface wind speed, sea surface temperature, total atmospheric water vapor content, and total cloud liquid water content turn out to be possible. Such an approach is especially adapted to weather systems characterized by storm wind speeds and moderate atmospheric absorption, such as winter extratropical cyclones and polar lows. The applicability of the new approach was demonstrated for the new radiometer AMSR-2 on board the GCOM-W1 satellite but can be extended to other radiometers. The inversion algorithms, trained on an ensemble of simulated brightness temperatures, are developed to retrieve SWS, SST, TWV, LWP, and for total atmospheric absorption at 10.65 GHz. For this frequency, the total upwelling radiation is still sensitive to the atmosphere but significantly less sensitive to LWP and especially to TWV variations. The trained algorithms for SWS and TWV retrievals, though not fully validated, were then used to demonstrate the potential of the retrieval results over pixels previously flagged.

[21] A larger data set of coregistered brightness temperatures and wind speed data will certainly be required from an ensemble of polar lows to establish more reliable statistics in these high wind speed conditions. Nevertheless, we believe that the inferred high wind products over larger ocean areas will clearly provide quantitative complementary surface wind information of interest for operational forecast models.

[22] Finally, τ_{10} is a new parameter in a list of AMSR-2-retrieved parameters to help global estimations of X band radio propagation for Earth/space slant path.

[23] **Acknowledgments.** Funding for this research was provided by the megagrant of the Russian Federation Government to support scientific research under the supervision of leading scientist at RSHU 11.G34.31.0078. GCOM-W1 AMSR-2 data were provided within the Research Agreement for the GCOM-W1 between the Japan Aerospace Exploration Agency and the V. I. Il'ichev Pacific Oceanological Institute FEB RAS. The support by the Russian Federal Programme under contract N14.B37.21.0619 and N2012-1.2.1-12-000-2007-078 is gratefully acknowledged.

[24] The Editor thanks two anonymous reviewers for their assistance in evaluating this paper.

References

Alishouse, J. C., J. B. Snider, E. R. Westwater, C. T. Swift, C. S. Ruf, S. A. Snyder, J. Vongsathorn, and R. R. Ferraro (1990), Determination of cloud liquid water content using the SSM/I, *IEEE Trans. Geosci. Remote Sens.*, *28*(5), 817–822.

Bobylev, L. P., E. V. Zabolotskikh, L. M. Mitnik, and M. L. Mitnik (2010), Atmospheric water vapor and cloud liquid water retrieval over the Arctic Ocean using satellite passive microwave sensing, *IEEE Trans. Geosci. Remote Sens.*, *48*(1), 283–294.

Japan Aerospace Exploration Agency (2005), AMSR-E Data Users Handbook, 3rd ed., Hatoyama, Japan.

Jung, T., E. Ruprecht, and F. Wagner (1998), Determination of cloud liquid water path over the oceans from Special Sensor Microwave/ Imager (SSM/I) data using neural networks, *J. Appl. Meteorol.*, *37*(8), 832–844.

Liebe, H. J., and D. H. Layton (1987), *Millimeter-Wave Properties of the Atmosphere: Laboratory Studies and Propagation Modeling*, Natl. Tech. Inf. Serv., Boulder, Colo.

Meissner, T., and F. J. Wentz (2004), The complex dielectric constant of pure and sea water from microwave satellite observations, *IEEE Trans. Geosci. Remote Sens.*, *42*(9), 1836–1849.

Meissner, T., and F. J. Wentz (2012), The emissivity of the ocean surface between 6 and 90 GHz over a large range of wind speeds and Earth incidence angles, *IEEE Trans. Geosci. Remote Sens., 50*(8), 3004–3026, doi:10.1109/ TGRS.2011.2179662.

Mitnik, L. M., and M. L. Mitnik (2003), Retrieval of atmospheric and ocean surface parameters from ADEOS-II Advanced Microwave Scanning Radiometer (AMSR) data: Comparison of errors of global and regional algorithms, *Radio Sci.*, *38*(4), 8065, doi:10.1029/ 2002RS002659.

Quilfen, Y., C. Prigent, B. Chapron, A. A. Mouche, and N. Houti (2007), The potential of QuikSCAT and WindSat observations for the estimation of sea surface wind vector under severe weather conditions, *J. Geophys. Res.*, *112*, C09023, doi:10.1029/2007JC004163.

Reul, N., J. Tenerelli, B. Chapron, D. Vandemark, Y. Quilfen, and Y. Kerr (2012), SMOS satellite L-band radiometer: A new capability for ocean surface remote sensing in hurricanes, *J. Geophys. Res.*, *117*, C02006, doi:10.1029/2011JC007474.

Turner, D. D., M. P. Cadeddu, U. Lohnert, S. Crewell, and A. M. Vogelmann (2009), Modifications to the water vapor continuum in the microwave suggested by ground-based 150-GHz observations, *IEEE Trans. Geosci. Remote Sens.*, *47*(10), 3326–3337.

Uhlhorn, E. W., P. G. Black, J. L. Franklin, M. Goodberlet, J. Carswell, and A. S. Goldstein (2007), Hurricane surface wind measurements from an operational stepped frequency microwave radiometer, *Mon. Weather Rev.*, *135*(9), 3070–3085.

Wentz, F. J., and T. Meissner (2000), Algorithm Theoretical Basis Document (ATBD), Version 2, AMSR Ocean Algorithm, RSS Tech. Proposal 121599A-1, Remote Sensing Systems.

Wentz, F. J., and R. W. Spencer (1998), SSM/I rain retrievals within a unified all-weather ocean algorithm, *J. Atmos. Sci.*, *55*(9), 1613–1627.